

the substrate molecule enhances its overall reactivity toward nucleophiles, which might be related to the quite high yields of carbene complexes in most reactions. However, orientation does not necessarily depend on those same factors that govern reactivity, as measured by the reaction rates or by the equilibrium constants.

The relative importance of charge and orbital controls can perhaps be examined by attempting nucleophilic additions to  $\text{CpMn}(\text{CO})_2\text{CSiMe}_3^+$ . The calculation shows the low-lying energetically isolated virtual orbitals to have Mn-C  $\pi$ -antibonding character, but there is also a high negative charge on the carbyne carbon atom (-0.70). Will any reaction occur? If it does, will it be addition to form a carbene complex or some other process? These questions can only be answered by appropriate experiments.

The generalization that reactions between hard acids and hard bases tend to be charge controlled whereas the reactions between soft species are more likely to be frontier controlled<sup>75</sup> does not hold in these reactions because there are hard as well as soft bases<sup>75</sup> among the nucleophiles that are found to effectively attack soft carbyne carbon.<sup>48-50</sup>

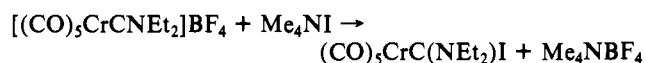
Triethylphosphine reacts with  $(\text{CO})_5\text{CrCNMe}_2^+$  to form *trans*- $\text{Et}_3\text{PCr}(\text{CO})_4\text{CNMe}_2^+$  at a higher temperature than that

used for reaction 2.<sup>19</sup> Schubert proposed a plausible explanation: the positive charge of the substrate compound is partly localized on the metal, thus decreasing the Cr-CO back-bonding so that the CO trans to the carbyne is replaced by phosphine, which has a higher  $\sigma$ -donor/ $\pi$ -acceptor ratio than CO does.<sup>8a</sup>

The importance of the reaction conditions is illustrated by the following two examples: Substitution<sup>19</sup> at -10 °C



Addition<sup>61</sup> at -60 °C



The orientation and selectivity in the reactions of carbyne complexes will continue to challenge experimentalists and theorists alike.

**Acknowledgment.** We are grateful to William B. Jensen of the University of Wisconsin in Madison for useful discussions and to Dr. Ulrich Schubert of the Technische Universität München and Professor Roald Hoffmann of Cornell University for sending us preprints of their articles. This research was supported by the National Science Foundation, Grant No. CHE7517744.

(75) Jensen, W. B. "The Lewis Acid-Base Concepts. An Overview"; Wiley: New York, 1980; pp 260-265.

## Dynamics of Light-Induced Water Cleavage in Colloidal Systems

Dung Duonghong, Enrico Borgarello, and Michael Grätzel\*

Contribution from the Institut de Chimie Physique, Ecole Polytechnique Fédérale, CH-1015 Lausanne, Switzerland. Received January 2, 1981

**Abstract:** A transparent  $\text{TiO}_2$  sol (particle radius 200 Å) is produced via hydrolysis of titanium tetraisopropoxide in acid aqueous solution. When loaded simultaneously with ultrafine Pt and  $\text{RuO}_2$  deposits, these particles display extremely high activity as water decomposition catalysts. Band-gap excitation of the  $\text{TiO}_2$  generates  $\text{H}_2$  with a quantum yield of  $30 \pm 10\%$ . Oxygen is produced in stoichiometric proportion. When  $\text{Ru}(\text{bpy})_3^{2+}$  or rhodamine B is used as a sensitizer, water is decomposed by visible light. Addition of methyl viologen ( $\text{MV}^{2+}$ ) increases significantly the  $\text{H}_2$  yield. Laser photolysis experiments performed with the  $\text{Ru}(\text{bpy})_3^{2+}/\text{MV}^{2+}$  system illustrate the high rate and specificity of the catalytic reactions leading to hydrogen and oxygen production from water.

The observation of light-induced oxygen evolution on illuminated  $\text{TiO}_2$  single crystals reported by Honda et al.<sup>1</sup> has stimulated extensive investigations<sup>2</sup> in the photoelectrochemical behaviour of this semiconductor. While developing mixed Pt/ $\text{RuO}_2$  catalysts for the mediation of water decomposition by visible light,<sup>3-9</sup> we

became intrigued with the outstanding performance of  $\text{TiO}_2$  particles as a support material. In the presence of a suitable sensitizer such a bifunctional redox catalyst affords sustained water cleavage over more than 20 days, the quantum yield being in excess of 5%. For understanding and further improvement of this system it is mandatory to perform detailed investigations on titania-based Pt/ $\text{RuO}_2$  catalysts of different composition and structure. On crucial parameter to be explored is the effect of particle size. It appears desirable to synthesize  $\text{TiO}_2$  particles of truly colloidal dimensions. As scattering effects are small, these solutions can be subjected to a detailed photochemical analysis by both conventional and flash photolysis techniques. Water decomposition studies with such transparent  $\text{TiO}_2$  sols are reported in this paper.

(1) (a) Fujishima, A.; Honda, K. *Bull. Chem. Soc. Jpn.* 1971, 44, 1148. (b) *Nature (London)* 1972, 238, 3m. (c) Inoue, T.; Fujishima, A.; Konishi, S.; Honda, K. *Ibid.* 1979, 277, 637.

(2) (a) Dutoit, E. C.; Cardon, F.; Gomes, V. P. *Ber. Bunsenges. Phys. Chem.* 1976, 80, 1285. (b) Fujishima, A.; Inoue, T.; Watanabe, T.; Honda, K. *Chem. Lett.* 1978, 357. (c) Gosh, A. K.; Maruska, H. P. *J. Electrochem. Soc.* 1977, 124, 1516. (d) Bard, A. J. *J. Photochem.* 1979, 10, 59. (e) Guruswamy, V.; Backris, J. O'M. *Sol. Energy Mater.* 1979, 1, 141. (f) Wrighton, M. S.; Ginley, D. S.; Wolczanski, P. T.; Ellis, A. B.; Morse, D. L.; Liwz, A. *Proc. Natl. Acad. Sci. U.S.A.* 1975, 72, 2858. (g) Rao, M. V.; Rajeshwar, K.; Pai Verneker, V. R.; Du Bow, J. *J. Phys. Chem.* 1980, 84, 1978. (h) Wagner, F. T.; Somorjai, G. A. *Nature (London)* 1980, 285, 559. (i) Schrauzer, G. N.; Gut, T. D. *J. Am. Chem. Soc.* 1977, 99, 7189. (j) Van Damme, H.; Hall, W. K. *Ibid.* 1979, 101, 4373.

(3) Kalyanasundaram, K.; Grätzel, M. *Angew. Chem. Int. Ed. Engl.* 1979, 18, 701.

(4) Kiwi, J.; Borgarello, E.; Pelizzetti, E.; Visca, M.; Grätzel, M.; *Angew. Chem., Int. Ed. Engl.* 1980, 19, 647.

(5) Borgarello, E.; Kiwi, J.; Pelizzetti, E.; Visca, M.; Grätzel, M. *Nature (London)* 1981, 289, 158.

(6) Grätzel, M. *Ber. Bunsenges. Phys. Chem.* 1980, 84, 981.

(7) Borgarello, E.; Kiwi, J.; Pelizzetti, E.; Visca, M.; Grätzel, M. *J. Am. Chem. Soc.*, accepted for publication.

(8) Grätzel, M. *Faraday Discuss. Chem. Soc.* 1980, No. 00.

(9) Kalyanasundaram, K.; Grätzel, M., Nato Summer School on Photoelectrochemistry, Nato Advanced Studies Treatise, Gent, Belgium, 1980.

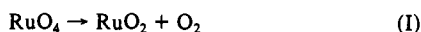
### Experimental Section

(i) **Materials.** Titanium tetraisopropoxide (Ventron GMBH), Ru(bpy)<sub>3</sub><sup>2+</sup> (Strem, dichloride), ruthenium tetroxide (RuO<sub>4</sub>, Alfa Inorganics) methyl viologen (BDH), H<sub>2</sub>PtCl<sub>6</sub> (Engelhard), and rhodamine B (Fluka, purum) were used as supplied.

The isopropyl ester derivative of Ru(bpy)<sub>3</sub><sup>2+</sup> (thereafter abbreviated as Ru(bpy)<sub>3</sub><sup>2+</sup>-IP) was synthesized by Dr. Patricia J. De Laive in our laboratory according to a procedure described earlier.<sup>10</sup> Deionized water was refluxed over alkaline permanganate and subsequently distilled three times in quartz vessels. All other reagents were at least analytical grade and were used as supplied.

(ii) **Preparation of Catalysts.** A 500-mg (or 1-g) sample of Ti(OCH(CH<sub>3</sub>)<sub>2</sub>)<sub>4</sub> was dissolved in 20 mL of 2-propanol. A 2 mL sample of this solution was slowly injected (microsyringe) into 20 mL of acidified water (pH 1.5, adjusted with HCl). A transparent solution of colloidal TiO<sub>2</sub> particles is thus obtained with a TiO<sub>2</sub> content of 500 mg/L (or 1 g/L) which is stable at pH ≤ 3.

The loading of TiO<sub>2</sub> with RuO<sub>2</sub> was carried out via decomposition of RuO<sub>4</sub> which occurs spontaneously according to eq 1.<sup>11</sup> A 0.5-mL sample



of a stock solution of RuO<sub>4</sub> in water (0.5 mg/mL) was injected into the 22-mL TiO<sub>2</sub> solution. An ultrafine<sup>12</sup> deposit of RuO<sub>2</sub> is formed under stirring for ca. 30 min. This process is catalyzed by light (RuO<sub>4</sub> absorbs around 400 nm) and may be further promoted by the 2-propanol present in the TiO<sub>2</sub> solution which could serve as a reductant of RuO<sub>4</sub>. The final RuO<sub>2</sub> concentration is 8 mg/L. For removal of excess 2-propanol, the solvent was evaporated in a Rotavap under vacuum and at 35 °C. The dried powder was redispersed in water by sonification. Complete removal of 2-propanol was checked carefully by subjecting the solution to GC analysis using a Poropack column (100 °C) and He as a carrier gas.

The final stage of catalyst preparation consisted in the loading of the TiO<sub>2</sub>/RuO<sub>2</sub> particles with Pt. Two different procedures were employed. In the first a solution of H<sub>2</sub>PtCl<sub>6</sub> was prepared and reduced with citrate in a separate container as described earlier.<sup>4,5,13-16</sup> The resultant ultrafine (particle diameter is <30 Å) platinum sol is subsequently mixed with the solution containing the TiO<sub>2</sub>/RuO<sub>2</sub> particles and sonicated. The second procedure consisted in photoplatinization:<sup>7,17</sup> H<sub>2</sub>PtCl<sub>6</sub> (3 mg and 1 mL of a 40% aqueous solution of formaldehyde) stabilized with methanol was added directly to 20 mL of the TiO<sub>2</sub>/RuO<sub>2</sub> solution (pH 1.5, TiO<sub>2</sub> content 0.5 g/L or 1 g/L, RuO<sub>2</sub> content 8 mg/L). After deoxygenation by flushing with nitrogen, the solution was irradiated in a Pyrex flask for 2 h with a 450-W Xe lamp. This suffices to quantitatively reduce the Pt ions by conduction band electrons of TiO<sub>2</sub> (holes created also under band-gap illumination are used to oxidize formaldehyde). The excess of formaldehyde as well as the methanol was subsequently removed under vacuum as described above. The dried TiO<sub>2</sub> powder has a loading of 80 mg of Pt and 16 mg of RuO<sub>2</sub>/1 g of TiO<sub>2</sub> or for the second batch 40 mg of Pt and 8 mg of RuO<sub>2</sub>/1 g of TiO<sub>2</sub>. The latter preparation was employed in the UV photolysis experiments. The two procedures of Pt loading yield catalysts of almost identical activity. However photoplatinization is preferred over citrate reduction since it is easier to perform and gives results of excellent reproducibility. Organic reductants can be avoided by exposing colloidal TiO<sub>2</sub> to UV light in the presence of both RuO<sub>4</sub> and H<sub>2</sub>PtCl<sub>6</sub>. This yields also excellent catalysts.

(iii) **Characterization of the Catalysts.** The size of the colloidal TiO<sub>2</sub> particles was determined by photon correlation spectroscopy. This technique has been described in detail earlier,<sup>18,19</sup> and only final results of the investigations will be presented here. Correlation functions were

(10) De Laive, P. J.; Whitten, D. G.; Giannotti, C. *Adv. Chem. Ser.* **1979**, No. 173, 236.

(11) The decomposition of RuO<sub>4</sub> according to eq 1 can be followed spectrophotometrically since the latter possesses a characteristic absorption around 400 nm. For details concerning RuO<sub>2</sub> formation from RuO<sub>4</sub> cf.: Connick, R. E.; Hurley, C. R. *J. Am. Chem. Soc.* **1952**, *74*, 5012.

(12) Light scattering experiments show that the particle size of TiO<sub>2</sub> increases by less than 5% upon RuO<sub>2</sub> deposition.

(13) Turkevich, J.; Aika, K.; Ban, L. L.; Okura, I.; Namba, S. *J. Res. Inst. Catal., Hokkaido Univ* **1976**, *24*, 54.

(14) Turkevich, J. In "Proceedings of Electrocatalysis of Fuel Cell Reactions", Brookhaven Symposium, 1978, p 123.

(15) Wilenzick, R. M.; Russell, D. C.; Morris, R. H.; Marshall, S. W. *J. Chem. Phys.* **1967**, *47*, 533.

(16) Brugger, P.-A.; Cuendet, P.; Grätzel, M. *J. Am. Chem. Soc.* **1981**, *103*, 0000.

(17) Kraeutler, B.; Bard, A. J. *J. Am. Chem. Soc.* **1978**, *100*, 4318.

(18) Corti, M.; Degiorgio, V. *Ann. Phys. (Paris)* **1978**, *3*, 303.

(19) Kiwi, J.; Grätzel, M. *J. Am. Chem. Soc.* **1979**, *101*, 7214. Monserrat, K.; Grätzel, M.; Tundo, P. *J. Am. Chem. Soc.* **1980**, *102*, 3689.

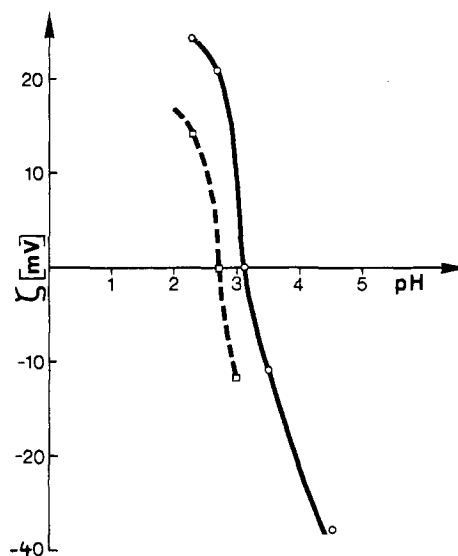


Figure 1.  $\zeta$  potentials of colloidal TiO<sub>2</sub> and colloidal TiO<sub>2</sub> loaded with Pt (80 mg/g of TiO<sub>2</sub>) and RuO<sub>2</sub> (16 mg/g of TiO<sub>2</sub>) (concentration of TiO<sub>2</sub> = 2 mg/L).

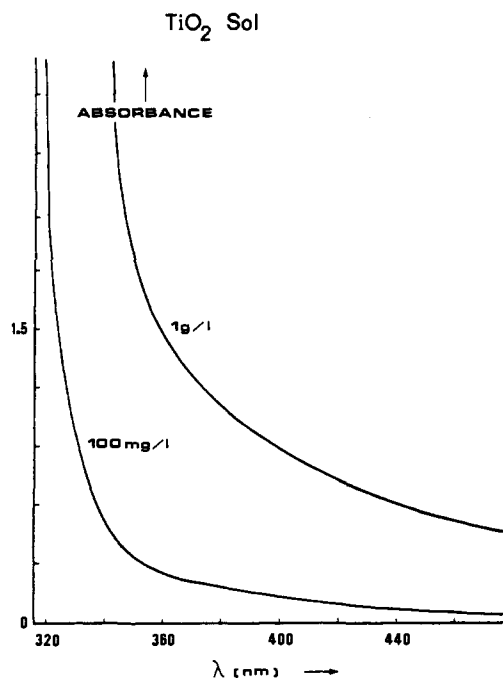


Figure 2. Visible and near UV absorption spectrum of the TiO<sub>2</sub> sol [TiO<sub>2</sub>] = 100 mg/L and 1 g/L; pH 1.5 adjusted with HCl).

obtained with a Chromatix light-scattering instrument.<sup>20</sup> They can be presented by a single exponential over at least two correlation times, indicating a surprisingly low degree of polydispersity. Application of the Stokes-Einstein equation yields a hydrodynamic radius of  $R_H = 200$  Å for TiO<sub>2</sub> alone and for the Pt and RuO<sub>2</sub> loaded particles  $R_H = 215$  Å.

The surface potential of the particles was determined by electrophoresis. A Rank Bros. Mark II instrument equipped with a He-Ne laser and a cylindrical cell configuration was employed. The laser beam is focused to a narrow volume of 90 μm<sup>3</sup> and the field of observation displayed on a TV camera. Through the combined effect of tiny probe volume, focused laser intensity, and high refractive index of TiO<sub>2</sub> ( $n = 2.7$ ), it is possible to identify scattering from individual particles. This allows for the direct observation of the particle migration over a distance of 105 μm. The mean electrophoretic velocity was determined by measuring the rate of migration at various distances from the cell wall ( $X$ ). The rates were fit to a polynomial in  $X$  and integrated over the whole tube radius. Division of the mean velocity by the field strength

(20) Chromatix Application Note LS-8 (1978), 560 Oakmed Parkway, Sunnyvale, CA 94086 (USA).

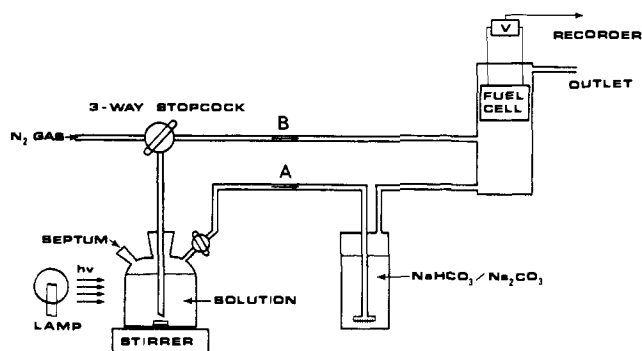


Figure 3. Experimental setup for the determination of light-induced oxygen evolution by the Teledyne-B<sub>1</sub> microfuel cell.

yields the mobility ( $\bar{\mu}$ ) which under our conditions<sup>21</sup> of particle radius and ionic strength is related to the  $\zeta$  potential via Henry's law

$$\zeta = \frac{4\pi\eta u}{\epsilon}$$

where  $\eta$  is the viscosity and  $\epsilon$  the dielectric constant.

$\zeta$  values obtained at different pH under maintaining constant ionic strength are displayed in Figure 1. The point of zero- $\zeta$  potential (ZPP) of the TiO<sub>2</sub> particles is obtained as 3.2. While the absolute values for  $\zeta$  are in good agreement with literature data, the ZPP is significantly below that observed for rutile and anatase powder.<sup>22</sup> On the other hand it is known that methods of preparation and pretreatment have a large effect on  $\zeta$  potential properties. For example oxyanions such as SO<sub>4</sub><sup>2-</sup> or PO<sub>4</sub><sup>3-</sup> are prone to specific adsorption on the surface of TiO<sub>2</sub> particles and can readily decrease the ZPP by more than 4 units. Though our medium contains only chloride ions which show little affinity for specific adsorption on TiO<sub>2</sub>, we believe that inclusion of some Cl<sup>-</sup> occurs during precipitation of the particles which would account for the observed shift in the ZPP.<sup>21</sup> Electrophoresis measurements carried out with the larger TiO<sub>2</sub> (anatase) particles employed in our earlier studies<sup>4-9</sup> gave a point of zero  $\zeta$  potential of around 5.

Figure 1 illustrates also that loading of TiO<sub>2</sub> by Pt and RuO<sub>2</sub> decreases the ZPP by ca. 0.3 unit. A trend in this direction is expected since the hydroxyl groups on the surface of RuO<sub>2</sub> and Pt are both very acidic. The ZPP for hydrated RuO<sub>2</sub> powder has recently been determined<sup>24</sup> as 2.3 and that for Pt is even below 2.

Further information concerning the structure of the colloidal TiO<sub>2</sub> particles was obtained from X-ray studies.<sup>25</sup> The diffraction patterns show the presence of anatase crystals, a significant portion of the material being X-ray amorphous.

These data are corroborated by results obtained from spectrophotometric measurements (Figure 2). The TiO<sub>2</sub> particles do not exhibit any absorption in the visible, the small base line drift being due to scattering. However, the absorption rises sharply at  $\lambda < 380$  nm. The onset agrees well with the 3.2-eV band gap of anatase. (According to Butler<sup>26</sup> the optical absorption coefficient near the band edge can be expressed by  $\alpha = A(h\nu - E_g)^{n/2}/h\nu$ , where  $n = 4$  for TiO<sub>2</sub>,<sup>27</sup>  $A$  is a constant,  $E_g$  is the energy of the band edge, and  $\nu$  is the frequency. This corresponds to a hyperbolic law in frequency near the band edge. At  $h\nu = E_g$  the extinction coefficient is zero).

(iv) **Apparatus.** Continuous illuminations were carried out with an Osram XBO 450-W Xe lamp equipped with a 15-cm water jacket to remove IR radiation. For visible light experiments a 400-nm cutoff filter was placed in the beam. The optical density of the filter is 3 at 395 nm. The solution volume was invariably 25 mL and was contained in a Pyrex flask equipped with optically flat entry and exit window. The filter effect of the Pyrex for UV light is significant. Thus the transmission of the entry window is 50% at 325 nm and practically zero below 300 nm. The UV light intensity was determined by using Aberchrome 540 as a chemical dosimeter.<sup>28</sup> A 25-mL sample of an Aberchrome solution

(21) In the colloidal system under investigation the Debye length ( $1/k$ ) is significantly smaller than the particle radius. Hence  $kr \gg 1$ . This justifies the application of Henry's equation to calculate  $\zeta$  potentials.

(22) (a) Parfitt, G. D. *Prog. Surf. Membr. Sci.* **1976**, *11*, 181. (b) Boehm, H. P. *Discuss. Faraday Soc.* **1971**, *52*, 264.

(23) We thank Professor H. P. Boehm for suggesting this possibility to us.

(24) Kiwi, J.; Grätzel, M. *Chem. Phys. Lett.*, in press.

(25) We are grateful to the X-ray analysis group of CIBA-GEIGY for performing these measurements on our samples.

(26) Butler, M. A. *J. Appl. Phys.* **1977**, *48*, 1914.

(27) Koffyberg, F. P.; Dwight, K.; Wold, A. *Solid State Commun.* **1979**, *30*, 433.

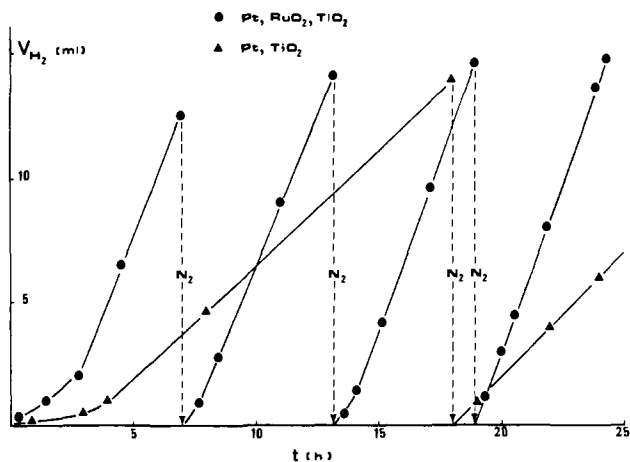


Figure 4. Water cleavage by near UV irradiation of TiO<sub>2</sub> dispersions (the volume of H<sub>2</sub> produced from irradiating 25-mL samples is plotted; N<sub>2</sub> indicates flushing the solution with nitrogen; room-temperature experiments): ●, Pt (1 mg), RuO<sub>2</sub> (0.2 mg), TiO<sub>2</sub> (25 mg); ▲, Pt (1 mg), TiO<sub>2</sub> (25 mg).

(concentration  $\geq 5 \times 10^{-3}$  M) were placed in the Pyrex flask and irradiated through an interference filter (Balzers, RUV 308) that passes essentially 310-nm light. The formation of the photoproduct ( $\phi = 0.2$ ) was monitored spectrophotometrically at 494 nm at various time intervals. The fluence absorbed by the solution was determined as  $1.5 \times 10^{15}$  quanta/s corresponding to  $2.5 \times 10^{-9}$  Einstein/s.

Laser photolysis experiments were carried out by using a frequency doubled JK-2000 Nd laser coupled with fast kinetic spectroscopy. Details of the setup have been published elsewhere.<sup>29</sup>

Hydrogen production was analyzed by gas chromatography. A GOW Mac system, carboxisieve column (35 °C) and N<sub>2</sub> as a carrier gas, was employed. An analogous procedure was employed for oxygen analysis. He instead of N<sub>2</sub> was used here as a carrier gas. Alternatively a Teledyne B<sub>1</sub> oxygen-specific microfuel cell was employed for oxygen analysis. This cell is placed in a cylindrical glass container which is connected to a flow system as shown in Figure 3. Prior to illumination the whole system is freed from oxygen by a stream of N<sub>2</sub>. The solution is then exposed to light. O<sub>2</sub> produced under illumination is transferred by the N<sub>2</sub> carrier gas to the cell where it is readily detected. The N<sub>2</sub> flow through the solution either is continuous or is intercepted during illumination by turning the three-way stopcock such that the N<sub>2</sub> passes through line B. This method proved to be reliable, specific, and highly sensitive and hence was applied in preference.

## Results and Discussion

(i) **Near-UV Light Photolysis.** Figure 4 shows data obtained from the photolysis of the aqueous TiO<sub>2</sub> sol loaded with Pt and simultaneously with Pt and RuO<sub>2</sub>. Conditions were Pt (1 mg), RuO<sub>2</sub> (0.2 mg), and TiO<sub>2</sub> (25 mg) in 25 mL of water of pH 1.5 adjusted with HCl. Hydrogen and oxygen are produced simultaneously under band-gap irradiation. For clarity of presentation only H<sub>2</sub> volumes are plotted. Oxygen strongly adheres to the TiO<sub>2</sub> particles and hence does not appear initially in the gas phase. Desorption occurs afterward. This effect will be dealt with in a subsequent paper. After a short induction period the H<sub>2</sub> generation rate in the case of the bifunctional redox catalyst establishes itself at 2.8 mL/h. The process was stopped after ca. 7 h when significant pressure had built up in the reaction vessel and the gas produced was flushed out with N<sub>2</sub>. Upon reillumination H<sub>2</sub> generation resumes at the initial rate. This cycle can be repeated many times. If after irradiation for 5 to 6 h the reaction mixture is stirred in the dark, recombination of hydrogen and oxygen occurs with a half-lifetime of 16 to 18 h. The back-reaction between H<sub>2</sub> and O<sub>2</sub> becomes also apparent when solutions are illuminated in the closed flask for longer periods (>15 h) where a photo-stationary state will eventually be reached.<sup>6</sup> These conditions were avoided in the present experiments which aimed at the

(28) This dosimetry was developed by Professor H. Heller at the University of Heller, G. U.S. Patent, 9719 254.

(29) Humphry-Baker, R.; Moroi, Y.; Grätzel, M.; Pelizzetti, E.; Tundo, P. *J. Am. Chem. Soc.* **1980**, *102*, 3689.

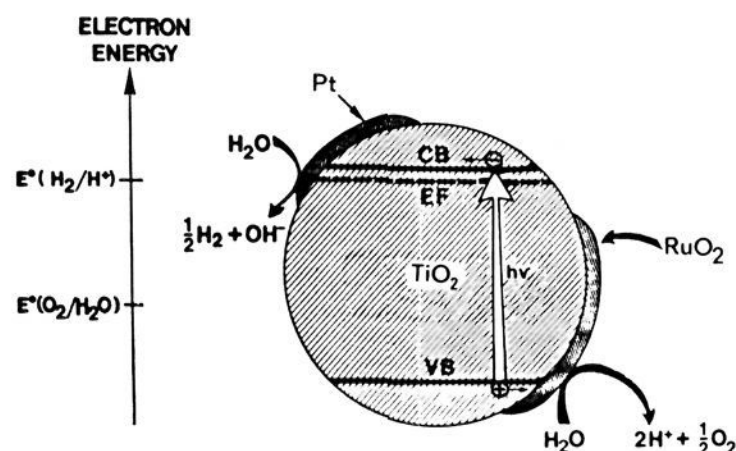


**Figure 5.** Schematic illustration of the photoinduced events leading to water decomposition.

determination of quantum yields. In Figure 4 the total amount of  $H_2$  produced is 56 mL (i.e.,  $2.5 \times 10^{-3}$  mol. This implies turnover numbers of at least 1700, 500, and 8 for the  $RuO_2$ , Pt, and  $TiO_2$  catalysts, respectively. In order to measure the quantum yield for  $H_2$  production, we repeated the experiment by illuminating through the Balzers RUV 308 interference filter. The value for  $\phi(H_2)$  is  $30 \pm 10\%$  at 310 nm.

Both  $RuO_2$  and Pt are required to obtain this surprisingly high quantum yield. In the absence of  $RuO_2$ <sup>30</sup> the  $H_2$  generation rates drops to 1 mL/h as shown in Figure 4. No water splitting at all could be observed if Pt or both Pt and  $RuO_2$  loading was omitted.

These results may be rationalized in terms of the model<sup>31</sup> presented in Figure 5. Band-gap excitation produces an electron-hole pair in the colloidal  $TiO_2$  particle. The electron is subsequently channelled to Pt sites where hydrogen evolution occurs. (This vectorial displacement of the electron may be assisted by an accumulation layer at the Pt/ $TiO_2$  interface which renders platinum positive with respect to  $TiO_2$ .) The flat-band potential of single crystal rutile electrodes has been measured as +0.1 V vs. NHE at pH 0.<sup>32</sup> This is below the thermodynamic limit required for hydrogen production from water. However  $V_{fb}$  of anatase is shifted cathodically by 200–300 mV<sup>33</sup> as a result of the larger band gap of anatase (3.2 eV, compared to 2.9–3 eV for rutile). The flat-band potential of anatase is ca. 300 mV more negative than that of rutile and hence is sufficiently cathodic to afford hydrogen production from water. Holes produced in the valence band of  $TiO_2$  are known to oxidize water even in the absence of  $RuO_2$  catalyst. However, the rate of this process is relatively slow. Gomes et al. reported<sup>34</sup> that hole capture on the surface of rutile by water is about  $8 \times 10^5$  times slower than that observed with an efficient hole scavenger such as sulfite ions. Apparently the role of  $RuO_2$  in our water splitting system is to accelerate the hole transfer from the valence band of  $TiO_2$  to the aqueous solution. The low overvoltage characteristic for oxygen evolution on  $RuO_2$ <sup>35</sup> renders hole capture by water particularly effective and hence inhibits electron-hole recombination.

In this context results obtained by Kawai and Sakata<sup>36</sup> with a catalyst consisting of a mechanically ground mixture of Pt,  $TiO_2$ ,

(30) While this work was in progress, a paper appeared (Sato, S.; White, J. M. *Chem. Phys. Lett.* **1980**, 72, 83) reporting photodecomposition of water over Pt/ $TiO_2$  catalysts. The stationary  $H_2$  evolution rate from 250 mg catalyst (quartz cell, 200-W high-pressure Hg lamp) is 2.2  $\mu$ L/h, i.e., about 1000 times smaller than that obtained with our bifunctional catalyst.

(31) This model is reminiscent of the concept of photochemical diodes: (a) Yoneyama, H.; Sakamoto, H.; Tamura, H. *Electrochim. Acta* **1975**, 20, 341. (b) Nozik, A. J. *Appl. Phys. Lett.* **1976**, 29, 150. (c) *Ibid.* **1977**, 30, 657. (d) Jarret, H. S.; Sleight, A. W.; Kung, H. H.; Gillson, J. L. *J. Appl. Phys.* **1980**, 51, 3916.

(32) Dutoit, E. C.; Cardon, F.; Gomes, W. P. *Ber. Bunsenges. Phys. Chem.* **1976**, 80, 475.

(33) See ref 2g and (a) Jaeger, D.; Bard, A. J. *J. Phys. Chem.* **1979**, 23, 3146. (b) Heller, A., Ed. "Semiconductor Liquid Junction Solar Cells"; The Electrochemical Society: Princeton, NJ, 1977; Chapter VII, p 272.

(34) Vanden Kerchove, F.; Vandermolen, J.; Gomes, W. P.; Cardon, F. *Ber. Bunsenges. Phys. Chem.* **1979**, 83, 230.

(35) Trasatti, S.; O'Grady, W. E. *Adv. Electrochem. Ser.*, in press. We are grateful to Professor Trasatti for making this manuscript available to us prior to publication.

(36) Kawai, T.; Sakata, T. *Nature (London)* **1980**, 286, 474.

## VISIBLE LIGHT EXPERIMENTS

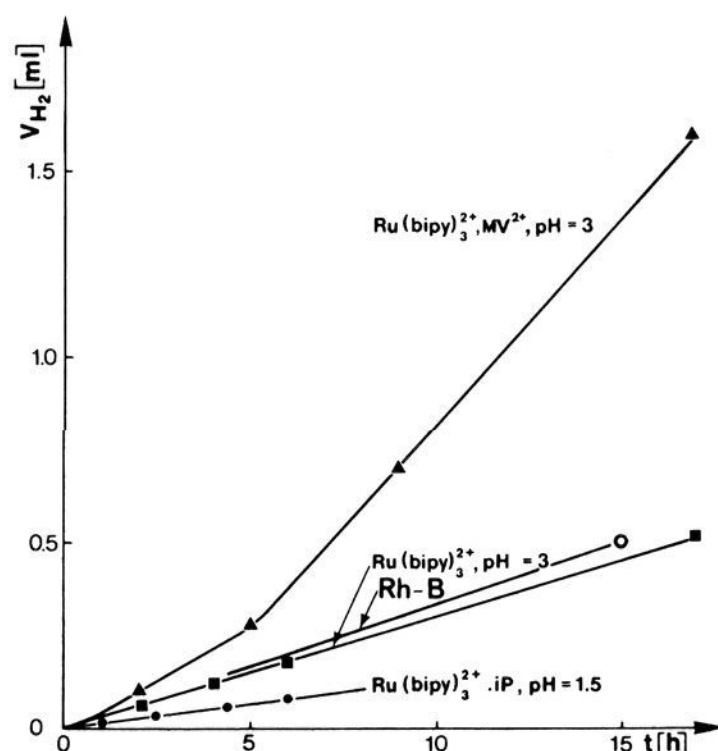


**Figure 6.** Water cleavage by visible light irradiation of aqueous solutions (room-temperature experiments, sensitizer concentration =  $2 \times 10^{-4}$  M,  $[MV^{2+}] = 5 \times 10^{-3}$  M).

and  $RuO_2$  should be mentioned.  $RuO_2$  was found to promote the light-induced oxidation of organic compounds such as sugars and alcohols. In this case the catalytic effect is due to enhancement of hole transfer from the  $TiO_2$  valence band to the reducing agent present in solution. Consistent with this interpretation are results we obtained from the UV photolysis of the Pt/ $RuO_2$ -loaded  $TiO_2$  sol in the presence of 2-propanol. The rate of  $H_2$  generation is here about 3 times faster than in 2-propanol-free solution, the quantum yield<sup>37</sup> of hydrogen production approaching 100%.

(ii) **Visible Light Photolysis.** We succeeded earlier<sup>3-9</sup> to decompose water by visible light by using  $Ru(bpy)_3^{2+}$  and its amphiphilic derivatives as sensitizers. Particularly effective in those systems was a  $TiO_2$ -based bifunctional redox catalyst<sup>4-7</sup> where the Pt/ $RuO_2$ -loaded  $TiO_2$  particles had been prepared by acid hydrolysis of  $TiOSO_4$  and doped with 0.4%  $Nb_2O_5$ . In view of these results it appeared interesting to examine the performance of the present  $TiO_2$  preparation in similar water decomposition systems. Results obtained from visible light photolysis experiments are plotted in Figure 6. The 400-nm cutoff filter placed in the light beam prevents entirely any direct band gap excitation of the  $TiO_2$  particles. Control experiments showed that not even a trace of hydrogen is obtained in sensitizer free solution under visible light illumination.

Consider first the lowest  $H_2$  evolution curve obtained at pH 1.5 with  $Ru(bpy)_3^{2+}$ -P as a chromophore. The choice of this sensitizer was based on its high redox potential ( $\sim 1.5$  V vs. NHE in water<sup>38</sup>) which makes oxygen formation from the oxidized sensitizer and water thermodynamically favorable even at a pH as low as 1.5. Water splitting is indeed observed albeit with small efficiency:  $H_2$  is produced at 0.012 mL/h. The simple ruthenium complex  $Ru(bpy)_3^{2+}$  fails to yield any  $H_2$  under illumination at pH 1.5. This is expected as the redox potential of the  $Ru(bpy)_3^{2+/3+}$  couple is only +1.2V<sup>39</sup> which provides insufficient driving force for water oxidation at pH 1.5. Water cleavage is obtained however at pH 3. Here stabilization of the  $TiO_2$  sol is required which in the absence of protective agent flocculates rapidly at the concentration employed (500 mg/L). The stabilizing agent used was polyvinyl alcohol (0.1% solution,  $M = 60\,000$ ).

(37) The maximum quantum efficiency for  $H_2$  production is 50%. In the presence of 2-propanol "current doubling" ncf. ref 2a) occurs due to electron injection from the 2-propanol radical in the  $TiO_2$  conduction band. This increases the quantum yield by at most a factor of 2.

(38) Kalyanasundaram, K.; Neumann-Spallart, M., unpublished results.

(39) Creutz, C.; Shutin, N. *Proc. Natl. Acad. Sci. U.S.A.* **1975**, 72, 2858.



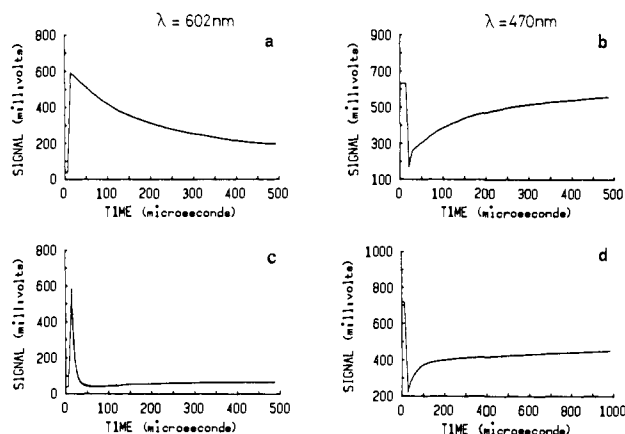


**Figure 7.** Oscilloscope traces obtained from the laser photolysis of  $10^{-4}$  M  $\text{Ru}(\text{bpy})_3^{2+}$  and  $2 \times 10^{-3}$  M  $\text{MV}^{2+}$  in deaerated aqueous solution of pH 1.5 (catalyst: Pt (40 mg/L)  $\text{RuO}_2$  (8 mg/L) loads on 500 mg of  $\text{TiO}_2/\text{L}$ ).

The rate of hydrogen generation is 0.03 mL/h with  $\text{Ru}(\text{bpy})_3^{2+}$  at pH 3. Interestingly, the simple triphenylmethane dye rhodamine B can replace  $\text{Ru}(\text{bpy})_3^{2+}$  as a sensitizer for water decomposition.<sup>40</sup> Irradiation of a  $5 \times 10^{-5}$  M solution of rhodamine B produces  $\text{H}_2$  at a rate of 0.04 mL/h.

The mechanism of water decomposition operative in this system involves injection of an electron from the excited state of the sensitizer into the conduction band of  $\text{TiO}_2$  leading to  $\text{H}_2$  evolution on Pt sites as discussed above. Only that part of the sensitizer can become photoactive that adheres to the particle surface or is contained within a diffusion layer<sup>41</sup> defined by the thickness  $d = (2D\tau)^{1/2}$ , where  $D$  is the diffusion coefficient and  $\tau$  the excited state lifetime. (For the ruthenium complex  $d$  is about 300 Å.) The propensity for charge injection increases with decreasing redox potential<sup>40</sup> of the excited state, i.e., in the order<sup>42</sup>  $\text{Ru}(\text{bpy})_3^{2+} \cdot 1\text{P} < \text{Ru}(\text{bpy})_3^{2+} < \text{Rh-B}$ . This and the affinity of the dye for adsorption at the  $\text{TiO}_2$ /water interface may have determined the trends in efficiency observed in Figure 6.<sup>43</sup> Another factor to consider is the rate of oxygen evolution from the dye cation and water. This process follows charge injection and takes place on  $\text{RuO}_2$  sites. Its rate will increase with pH and the ground-state redox potential of the sensitizer.

After now to Figure 6, we note that for  $\text{Ru}(\text{bpy})_3^{2+}$  the hydrogen generation rate increases significantly upon addition of methyl viologen ( $\text{MV}^{2+}$ ) to the solution. After an induction period  $\text{H}_2$  is formed at 0.14 mL/h. This rate can be sustained over at least several days, turnover numbers for  $\text{Ru}(\text{bpy})_3^{2+}$  and  $\text{MV}^{2+}$  being in excess of 400 and 20, respectively.

An enhancement of the rate of water decomposition by  $\text{MV}^{2+}$  has been observed before with a different Pt/ $\text{RuO}_2$ / $\text{TiO}_2$  catalyst<sup>7</sup> and must be attributed to the electron-transfer quenching<sup>44</sup> of  $\text{Ru}(\text{bpy})_3^{2+}$  excited states by  $\text{MV}^{2+}$ .



This could render photoactive  $\text{Ru}(\text{bpy})_3^{2+}$  species present in the solution bulk and away from the particle surface. However re-

(40) The redox potential of rhodamin B is  $-0.7$  V vs. NHE in the excited state and  $+1.3$  V in the ground state. For  $\text{Ru}(\text{bpy})_3^{2+} \cdot 1\text{P}$  and  $\text{Ru}(\text{bpy})_3^{2+}$  the excited-state potentials are  $-0.5$  and  $-0.85$  V (NHE), respectively. (cf. Sutin, N.; Creutz, C. *Adv. Chem. Ser.* 1978, No. 168, 1).

(41) Gosh, P. K.; Spiro, T. G. *J. Am. Chem. Soc.* 1980, 102, 5543.

(42) The flatband potential of  $\text{TiO}_2$  shifts cathodically by about  $-90$  mV when increasing the pH from 1.5 to 3. This offsets partially the difference in reducing power between  $^*\text{Ru}(\text{bpy})_3^{2+} \cdot 1\text{P}$  and  $^*\text{Ru}(\text{bpy})_3^{2+}$ .

(43) We wish to draw attention to a recent paper on the sensitization of  $\text{TiO}_2$  particle catalysts by phthalocyanines. The reaction investigated was oxygen reduction by hydroquinones. Fan, Fu-Ren, F.; Bard, A. J. *J. Am. Chem. Soc.* 1979, 101, 6139.

(44) This reaction was first investigated by Whitten et al. (Bock, C. R.; Meyer, T. J.; Whitten, D. G. *J. Am. Chem. Soc.* 1974, 96, 4710) after Gafney and Adamson discovered that the excited Ru complex can serve as a powerful one-electron reductant (Gafney, H. D.; Adamson, A. W. *J. Am. Chem. Soc.* 1972, 94, 8238).

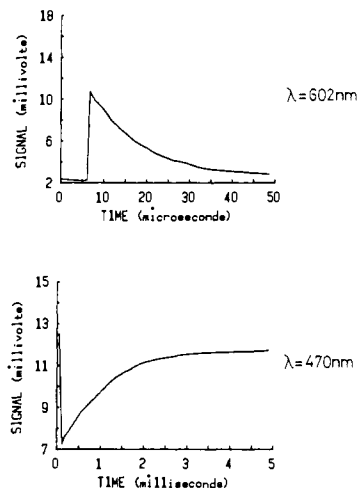
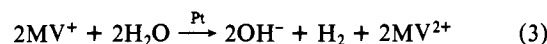
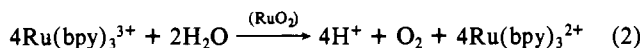


**Figure 8.** Oscilloscope traces obtained from the laser photolysis conditions as in Figure 7 except pH 3.

action 1 can only contribute to water decomposition if the subsequent dark reaction<sup>45</sup> with the redox catalysts, i.e.



are very fast and moreover specific. The present transparent  $\text{TiO}_2$  sol lends itself to a laser investigation which will clarify these points.

(iii) **Laser Photolysis Investigation.** Results obtained from the 530-nm laser photolysis of aqueous solutions containing  $10^{-4}$  M  $\text{Ru}(\text{bpy})_3^{2+}$  and  $2 \times 10^{-3}$  M  $\text{MV}^{2+}$  are depicted in Figure 7. The absorbance at 470 and 602 nm reflects the kinetic behavior of  $\text{Ru}(\text{bpy})_3^{3+}$  and  $\text{MV}^+$ , respectively. Consider first parts a and b of Figure 7 which were taken in the absence of catalyst. The redox reaction (1) takes place immediately after the laser pulse and produces a steep rise in the 602-nm absorbance due to the formation of  $\text{MV}^+$  and a bleaching at 470 nm. The decay of the 602-nm absorption as well as the bleaching recovery follow both the same second-order kinetics, the first half-lifetime being  $\sim 250$   $\mu\text{s}$ . Addition of catalyst (20 mg of Pt/8 mg of  $\text{RuO}_2$ /500 mg of  $\text{TiO}_2/\text{L}$ ) produces a drastic enhancement of the  $\text{MV}^+$  decay which now follows first-order kinetics. The half-lifetime is here only 3.5  $\mu\text{s}$  corresponding to a pseudo-first-order rate constant of  $2 \times 10^5$   $\text{s}^{-1}$ . In striking contrast to this behavior stands the effect of the catalyst on the bleaching events at 470 nm. The bleaching recovery is markedly retarded by the addition of catalyst, indicating an increased lifetime of  $\text{Ru}(\text{bpy})_3^{3+}$ .

Several important points should be stressed in discussing the data of Figure 7. First, we note that with this colloidal catalyst it is possible to intercept the back-reaction very efficiently at surprisingly low Pt concentration. The rate constant for reaction 3 is calculated to be  $k = 2 \times 10^9$   $\text{M}^{-1} \text{s}^{-1}$  if the analytical Pt concentration is used ( $10^{-4}$  M). However, this gives certainly only a lower limit as Pt is present in aggregated and not monoatomic form. As the aggregation number of Pt is probably greater than 100, the true rate constant referring to the Pt particle concentration exceeds  $2 \times 10^{11}$   $\text{M}^{-1} \text{s}^{-1}$ . As this value exceeds significantly the diffusion controlled limit, one is led to invoke participation of the  $\text{TiO}_2$ -support material in the catalytic event. Apparently the  $\text{TiO}_2$  particles can themselves act as an electron-acceptor relay, thereby increasing significantly the cross-section of the Pt reaction with  $\text{MV}^+$ . This mediator function exerted by the colloidal  $\text{TiO}_2$  is due to electron injection from  $\text{MV}^+$  into the  $\text{TiO}_2$  conduction band. From there on the electron is channeled to Pt sites where  $\text{H}_2$  evolution occurs. A further point to be dealt with is the achievement of specificity with this bifunctional redox catalyst.

(45) References concerning the catalysis of  $\text{H}_2$  and  $\text{O}_2$  production from water in sacrificial systems are given in ref 6.

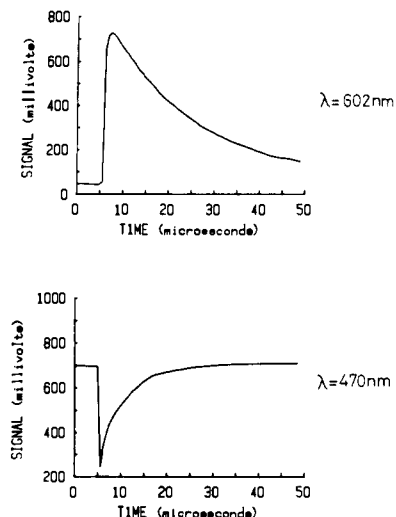


**Figure 9.** Oscilloscope traces from laser photolysis experiments conditions as in Figure 7 except pH 6.5 (the catalyst used was  $\text{RuO}_2$  (8 mg/L) loaded on  $\text{TiO}_2$  (500 mg/L)).

Comparison of parts c and d of Figure 7 shows that at pH 1.5 only the reaction of  $\text{MV}^+$  is catalyzed. Water oxidation by  $\text{Ru}(\text{bpy})_3^{3+}$  according to eq 2 is slow at this pH and does not play any role on the time scale of observation.<sup>46</sup> (In fact if  $\text{RuO}_2$  is absent, i.e., the  $\text{TiO}_2$  particles loaded by Pt alone are used as catalysts, the same bleaching kinetics are observed as in Figure 7d.) The slow rate of reaction 2 at pH 1.5 explains the failure of  $\text{RuO}_2$  to effect water decomposition under these conditions.

Figure 8 shows oscilloscope traces obtained at pH 3 where water cleavage is operative. While the rate of the  $\text{MV}^+$  decay is somewhat slower than at pH 1, that of the bleaching recovery is greatly increased. This is attributed to  $\text{RuO}_2$ -catalyzed water oxidation. The pseudo-first-order rate constant obtained for this process is  $\sim 10^3 \text{ s}^{-1}$ . This rate is significantly higher than  $k \approx 0.1 \text{ s}^{-1}$  observed by Pelizzetti et al.<sup>47</sup> for water oxidation by  $\text{Fe}(\text{bpy})_3^{3+}$ . In the latter study a  $\text{RuO}_2$  sol protected by a copolymer of styrene and maleic anhydride was used as a catalyst.

We finally examined solutions containing colloidal  $\text{TiO}_2$  particles loaded only with  $\text{RuO}_2$  by laser photolysis. Oscilloscope traces are presented in Figure 9. We note here a reversal of the features obtained with the bifunctional or Pt-loaded  $\text{TiO}_2$  particles. The bleaching at 470 nm recovers very rapidly according to a first-order law with a rate constant of  $1.4 \times 10^5 \text{ s}^{-1}$ . The 602 nm decay by contrast is relatively slow, the specific rate being  $4 \times 10^4 \text{ s}^{-1}$ . The decrease in the  $\text{MV}^+$  absorption reflects mainly the

kinetics of charge injection in the  $\text{TiO}_2$  conduction band. Thus the lifetime of  $\text{MV}^+$  is ca. 40  $\mu\text{s}$  in colloidal  $\text{TiO}_2$  solution which are Pt and  $\text{RuO}_2$  free while the lifetime of  $\text{Ru}(\text{bpy})_3^{3+}$  under these conditions is several hundred microseconds. From this asymmetric behavior of the 470- and 602-nm absorption it is inferred that the reaction of  $\text{Ru}(\text{bpy})_3^{3+}$  with  $\text{RuO}_2$  is much faster<sup>48</sup> than that of  $\text{MV}^+$ . This finding is important in that it illustrates the specificity of interaction of this catalyst with the oxidized sensitizer.

### Conclusions

The present investigation introduces a bifunctional colloidal semiconductor,  $\text{TiO}_2$ , as a catalyst in water splitting systems. Direct band-gap excitation produces  $\text{H}_2$  and  $\text{O}_2$  with an efficiency approaching the maximum possible yield, i.e., 50%. This may seem surprisingly high in view of the fact that  $\text{H}_2$  and  $\text{O}_2$  are produced as a gas mixture. An immediate conclusion is that oxygen does not interfere to a great extent in the water-cleavage process. One interaction of concern is  $\text{O}_2$  reduction on the Pt sites which would compete with hydrogen evolution and hence decrease the quantum efficiency of the device. Although  $\text{O}_2$  reduction is slow on Pt macroelectrodes (the exchange current density is  $\sim 10^{-11} \text{ A/cm}^2$  as compared to  $\sim 10^{-3} \text{ A/cm}^2$  for water reduction<sup>49</sup>), a large overpotential is evidently available to drive this reaction. However, the kinetics may be different on the ultrafine Pt deposits and oxygen adsorption to the  $\text{TiO}_2$  carrier could further impair this undesired cross reaction. A key role to achieve high efficiency is played by the  $\text{RuO}_2$  deposit which greatly facilitates the transfer of holes from the valence band of the semiconductor to the solution bulk.

As for the visible light experiments the performance of the present system as far as quantum yield of water splitting is concerned is far from matching that of earlier catalytic systems<sup>4-8</sup> in which somewhat larger anatase particles doped with  $\text{Nb}_2\text{O}_5$  were employed. Evidently further investigations are required to establish the role of n doping of the colloidal particles. In this paper we restricted ourselves to demonstrate how the catalyst operates in a system that gives  $\text{H}_2$  and  $\text{O}_2$  from visible light. Unambiguous evidence is presented that the catalyst intervenes extremely rapidly and moreover specifically in the redox events leading to water splitting.

**Acknowledgment.** We are grateful for support of this work by the Swiss National Foundation (Grant 2.168.0.78), CIBA-GEIGY AG (Basel, Switzerland), and Engelhard Industries, Metro Park, NJ. Thanks are due to Dr. R. Humphry-Baker for skillful assistance with the electrophoresis measurements and to Professor E. Pelizzetti, University of Torino, Italy, for stimulating discussions.

(48) The reaction of  $\text{Ru}(\text{bpy})_3^{3+}$  with water in the presence of  $\text{RuO}_2$  appears to be catalyzed by  $\text{OH}^-$  in the pH domain investigated.

(49) Van den Brink, F.; Barendrecht, E.; Visscher, W. *Recl. Trav. Chim. Pays-Bas* **1980**, *99*, 253.

(46) Kiwi, J.; Grätzel, M. *Chimia* **1979**, *33*, 289.

(47) Pramauro, E.; Pelizzetti, E. *Inorg. Chim. Acta Lett.* **1980**.